

DISLOCATION-STACKING FAULT TETRAHEDRON INTERACTION: WHAT WE CAN LEARN FROM ATOMIC SCALE MODELING—Yu. N. Osetsky, R. E. Stoller, and Y. Matsukawa (Oak Ridge National Laboratory)*

OBJECTIVE

The objective of this study is to understand atomic-scale details of interaction of a moving dislocation with Stacking Fault Tetrahedra (SFTs) in irradiated and aged fcc metals.

SUMMARY

Stacking fault tetrahedra (SFTs) are formed under irradiation of fcc metals and alloys with low stacking fault energy. The high number density of SFTs observed suggests that they should contribute to radiation-induced hardening, and, therefore, taken into account when estimating mechanical properties changes of irradiated materials. The central issue is describing the individual interaction between a moving dislocation and an SFT, which is characterized by a very fine size scale on the order of a few to one-hundred nanometers. This scale is amenable to both in-situ TEM experiments and large-scale atomic modeling. In this paper we present results of an atomistic simulation of dislocation-SFT interactions using molecular dynamics (MD). The MD simulations modeled an edge dislocation interacting with SFTs with different sizes and at different temperatures and strain rates. The results are compared with observations from in-situ deformation experiments in which several interactions between moving dislocations and SFTs were observed. It is demonstrated that in some cases the simulations and experimental observations are quite similar, suggesting a reasonable interpretation of experimental observations. Other cases, when modelling does not reproduce experimental observations, are also discussed and the importance of strain rate, dislocation nature and specimen surface effect are indicated.

Introduction

Stacking fault tetrahedra (SFTs) are common defects induced by different treatments, such as irradiation, ageing after quenching and deformation, in metals with a low level of stacking fault energy (SFE) [1-3]. In many cases these defects are mainly responsible for strengthening, hardening and plastic instability during deformation. Interactions between dislocations moving through the population of the existing SFTs is in the basis of these effects and therefore it is important to understand their mechanisms. Three different approaches, namely experiment, continuum theory and atomistic modeling, are currently used to study the details of dislocation – SFTs interactions. The experimental techniques employ in-situ experiments in which the specimen subjected to transmission electron microscopy (TEM) is deformed simultaneously. Provided the resolution is high enough, many important details of the interaction can be revealed in such experiments [4,5]. The disadvantage of the experimental methods is low spatial and time resolution, of about few tens of nm and one image per 1/30 sec. This limits observation of only large defects and very low rate of deformation. The continuum theory approach can be used to investigate dislocation-dislocation type reactions which can be applied to SFTs that are large enough to be described as a set of stair rod dislocations [6]. This approach can be applied to large SFT, with an accuracy limited to the details of the dislocation-dislocation interaction considered at continuum level. Temperature and strain rate effects cannot be studied with this approach. And finally, atomic scale modelling can be formally used to investigate all aspects of dislocation-SFT interactions [7,8,9]. The main limitation of atomic-scale simulation is the total time of the interaction because it is limited by a few nanoseconds. Nevertheless, modern atomic-scale models can be used to obtain valuable information on dislocation-SFT interactions, which in some cases can be compared directly with in-situ experiments. In the present paper we report first results of an extended programme of atomic-scale modelling of dislocation dynamics in the environment of high density of small, less than ~6nm, SFTs which are formed under irradiation by energetic particles. This study is part of a multi-scale materials modeling program aimed understanding the effects of irradiation on the mechanical properties of fusion materials.

*Paper submitted to the Journal of Nuclear Materials.

Model

Interactions between a moving edge dislocation and SFT have been studied using the atomistic model developed in ref. [10]. The model was applied for two, qualitatively different, conditions namely statics, e.g., zero temperature, and dynamics, e.g., finite temperature and strain rate. The first approach allows investigation of the equilibrium state of a system containing a dislocation and an obstacle at a certain strain. Only this type of atomic-scale modeling can be compared directly with the continuum dislocation dynamics, and this can be used for parameterization of dislocation-obstacle interaction mechanisms. The second approach allows investigation of temperature and strain rate effects, which are far beyond the continuum theory. The main advantage of the model developed in ref. [10] is that stress-strain dependences, and therefore the critical resolved shear stress (CRSS), can be obtained under different conditions. In the present work we have simulated fcc crystal of size 46.0 x 35.5 x 25.7 nm along the $[1\bar{1}0]$, $[11\bar{2}]$ and $[111]$ axes respectively and containing about 3,5 million mobile atoms interacting via a many-body potential parameterized for copper in [11].

The edge dislocation with initial Burgers vector of $\frac{1}{2}[1\bar{1}0]$ and a (111) glide plane was first introduced, then relaxed. During relaxation the dislocation dissociated into two Shockley partials separated with a stacking fault of about 3nm of width. Stacking fault tetrahedra of size from 2.5nm to 4.1nm were then created in the vicinity of the dislocation so that the dislocation glide plane intersects the SFT at different levels. In static modeling at $T=0K$, strain was incrementally increased by 10^{-4} per step with the following relaxation of the system to the minimum of potential energy. In dynamic modelling at $T>0K$ strain rate in the range $(2-10)\times 10^6 s^{-1}$ was applied. For the crystals simulated such strain rate results in dislocation velocity from ~ 3 to ~ 40 m/s. More details on model crystal loading can be found in ref. [10]. Stress-strain dependences, the dislocation and the SFT configurations were analyzed and visualized during both types of modeling.

Due to space limitations we present here only the results obtained for the case of 4.1nm SFT containing 136 vacancies. This SFT was cut by a moving dislocation at different levels schematically presented in Fig. 1 where h is the distance between the dislocation glide plane and the SFT base. Note that the height of the tetrahedron is equal to ~ 3.34 nm.

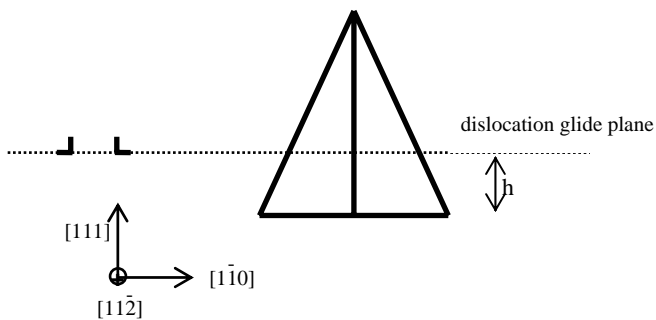


Fig. 1. Schematic view of dislocation-SFT interaction geometry.

Results

An example of stress-strain curves obtained for the case $h=0.96$ nm at different temperatures is presented in Fig. 2. One can see that the critical resolved shear stress, which is the maximum stress level in each curve, depends strongly on temperature. It drops from ~ 253 MPa at $T=0$ to 148MPa at $T=10K$ and to ~ 75 MPa at $T=300K$. Note that a significant drop occurs at very low temperatures implying that even very small atomic vibrations significantly assist the dislocation in penetrating through the SFT.

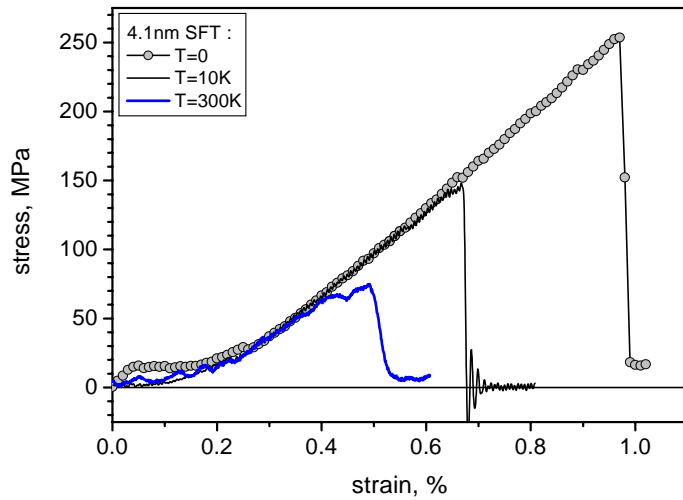


Fig. 2. Applied stress as function of strain in crystal at $T=0, 10$ and 300K containing a dislocation gliding through a row of 4.1nm (136 vacancies) SFT at $h=0.96\text{nm}$

The stress-strain behavior depends also upon h as shown in Fig. 3 for $T=10\text{K}$ where h starts at -0.48nm (just below the SFT base) for curve 1 and ends at $h=2.40\text{nm}$ for curve 7. The maximum CRSS, 182MPa , was observed for the case $h=0$, e.g., when the dislocation glide plane coincides with the SFT stacking fault. It is interesting to note that the CRSS is rather low for the first case on Fig. 3, when the dislocation glide plane is just

below the SFT's stacking fault. The dependence of the CRSS versus h is presented in Fig. 4. The overall conclusion is that the CRSS increases as the dislocation glide plane approaches the SFT base inside the SFT volume. At this position dislocation is more strongly pinned and the critical leaving angle decreases. The example of the dislocation configuration at critical stress, $\sigma=148\text{MPa}$, for the case $h=0.96$ at 10K is presented in Fig. 5. The grey circles indicate atoms with high potential energy and a low coordination number, therefore belonging to the dislocation core. The shape of the dislocation (circles) and stacking fault area (small crosses) are readily seen, and it is clear that estimating the critical angle is rather difficult due to dissociation of the dislocation.

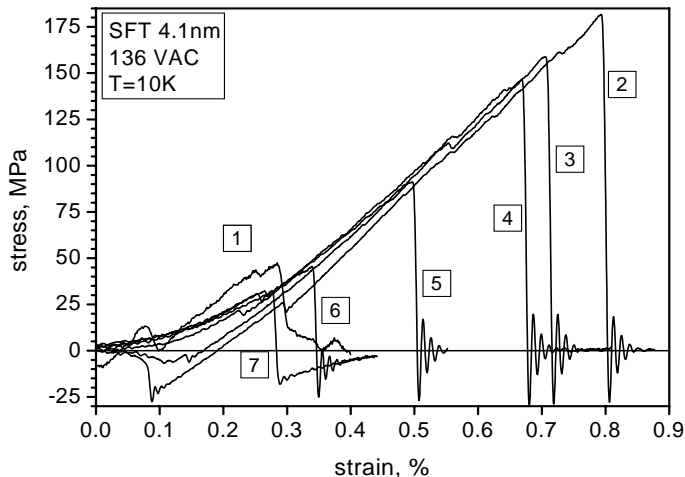


Fig. 3. Applied stress as function of strain in crystal at $T=10\text{K}$ containing a dislocation gliding through a row of 4.1nm SFT at different h : 1 – $h = -0.48\text{nm}$, 2 – $h=0$, 3 – $h = 0.48\text{nm}$, 4 – $h = 0.96\text{nm}$, 5 – $h = -1.44\text{nm}$, 6 – $h = 1.92\text{nm}$ and 7 – $h = 2.4\text{nm}$.

The position of the dislocation as it hits the SFT defines also the structural change of the SFT. In other words, the mechanism of the dislocation-SFT interaction depends on the geometry of the interaction. Thus, if the

dislocation hits the SFT close enough to its vertex, the SFT may not be damaged – the upper part of the SFT is shifted when the leading partial dislocation pulls away but after the trailing partial dislocations leaves the SFT it recovers its perfect configuration by a collective shift of the corresponding atoms above the glide plane. Note that such a recovery of the SFT was observed when distance between the glide plane and the vertex is $\leq 1.5\text{nm}$. If it is larger the SFT can be damaged in different ways depending on h . Some configurations of SFTs after interaction with the dislocation are presented in Fig. 6. In these figures the size of the cube box is $13a$ ($a=0.3615\text{nm}$ is Cu lattice parameter) and the grid size is $1a$. In general the damage to an SFT includes formation of two ledges of opposite sign on two faces. An I-type ledge is created on the face where the leading partial dislocation entered the SFT and a V-type ledge is created

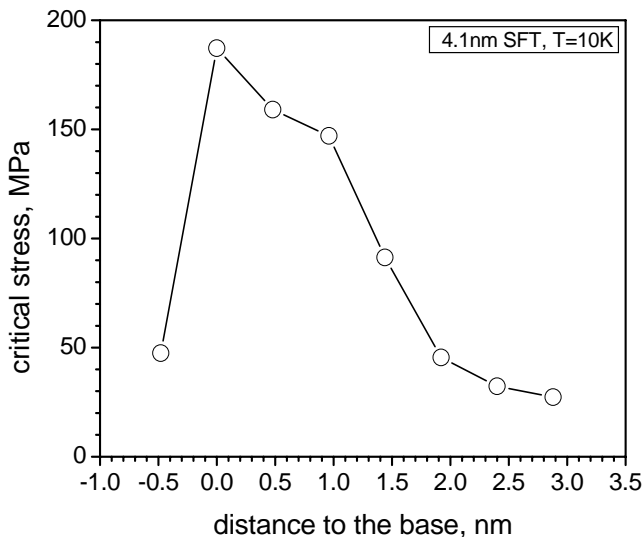


Fig. 4. Dependence of the value of critical resolved shear stress against distance between the dislocation glide plane and the base of a 4.1nm SFT simulated at T=10K.

on the face where the trailing partial dislocation left it. The detailed configuration of ledges depends on h as it can be seen in Fig. 6b-c. on h as it can be seen in Fig. 6b and c. The case $h=0$, when the whole upper part of the SFT was shifted relatively the stacking fault of the lower base, can be interpreted as a creation of the minimum size ledges (see Fig. 6d).

Experimentally observed formation of channels cleared from radiation-induced

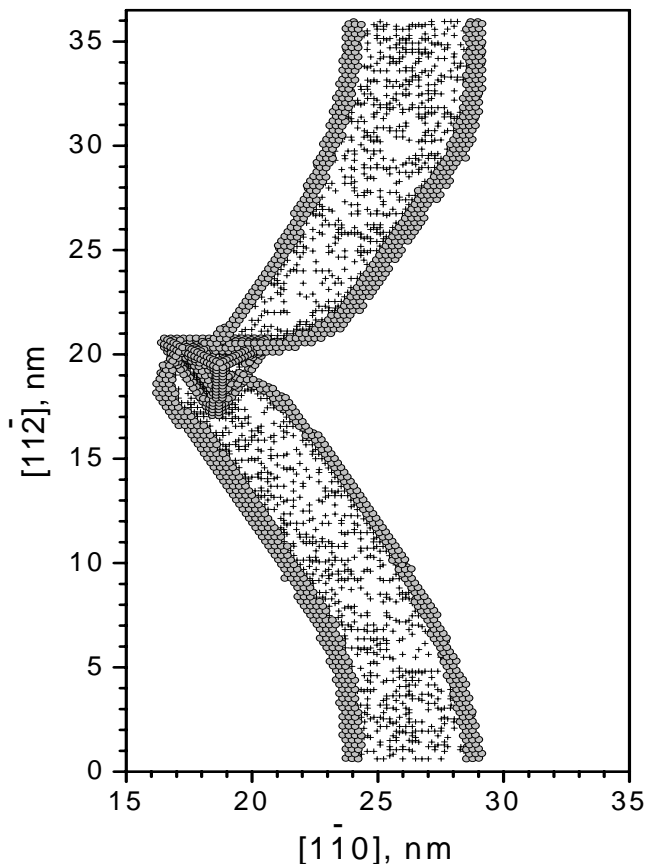


Fig. 5. Dislocation line in the (111) slip plane at the critical stress for 4.1nm SFT cut at $h=0.96\text{nm}$ at T=10K. Gray circles are atoms with high energy and low coordination number, little crosses are atoms which are definitely in HCP environment.

defects is characterised by many dislocations formed from the same source gliding in the same and close slip planes [12]. That means the same obstacle, i.e. SFT, can be cut many time by dislocations in the same and/or close slip planes. We have investigated such cases and found that the result again depends on h . For large h , e.g., when slip plane is close to the vertex, SFT cannot be damaged and it restores perfect configuration after every dislocation passes through. In the case of small h , when ledges can be formed, the SFT can be broken into pieces separated proportionally of the number of dislocations passed. An example of configuration of a 2.5nm SFT, containing 45 vacancies, after multiply dislocation cut is presented in Fig. 7.

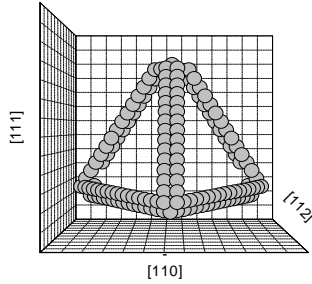
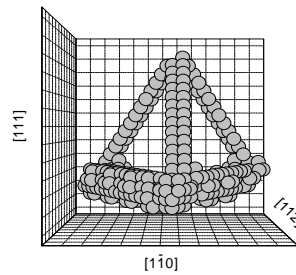
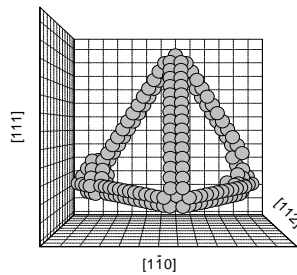
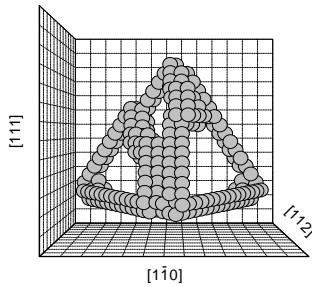


Fig. 6. Configuration of 4.1nm SFT a) before and b)-d) after interaction with the dislocation gliding at different h : b) $h = 0.96\text{nm}$, c) $h = 0.48\text{nm}$ and d) $h = 0$.



The first dislocation, Fig. 7-1 (the number of the configuration in Fig. 7 indicates how many dislocations passed through), created a pair of ledges described above whereas next dislocations shift the upper part of the SFT towards the Burgers vector direction. In the case described the dislocations move from the right to the left. The fourth dislocation separates completely a small perfect SFT containing 21 vacancies and a 24 vacancies cluster with two parallel stacking faults, one of which is the former SFT base and the other one is created due to interaction. We did not identify the structure of the lower cluster but it is definitely that of low binding energy and, therefore, should be either dissociated or transformed, e.g., to Frank loop, depending on time and temperature. It is interesting to note that the upper part of the SFT is undamaged and this is consistent with experimental TEM observations during in-situ deformation of quenched and annealed gold [5].

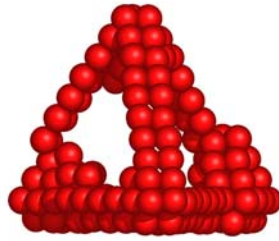
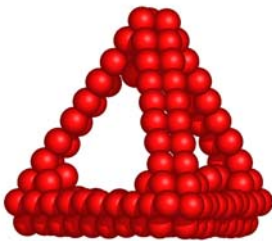
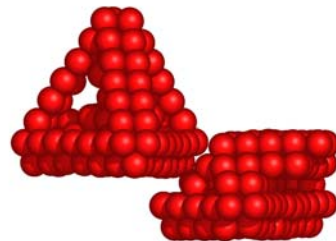
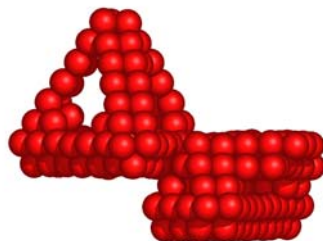
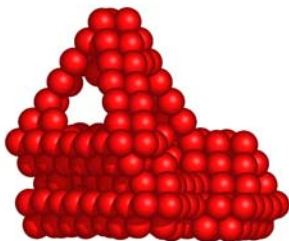


Fig. 7. Configuration of 2.5nm (45 vacancies) SFT 0) before and 1)-4) after interactions with the dislocation gliding through its centre. The number near each configuration indicates how many time the dislocation passed through.



Conclusions and Future Work

Interaction between a moving edge dislocation and stacking fault tetrahedra of size from 2.5 to 4.1 nm has been studied at atomic scale by molecular dynamics and statics techniques. It was found that the critical resolved shear stress depends strongly upon the geometry of the interaction and the crystal temperature. In general, CRSS decreases at higher temperature and larger distance, h , between the dislocation glide plane and the SFT base parallel to it. Depending on h , the SFT can be damaged, or not. The damage includes creation of two ledges of opposite signs on the SFT's faces cut by the moving dislocation. Creation of ledges decreases the SFTs stability and can serve as an initiation of their dissolution. The latter is observed commonly in in-situ deformation TEM experiments [4,5]. However, more detailed study is necessary for a full understanding of the atomic-scale mechanisms involved. Note, that in general the damage of SFTs depends on its size and structure. Thus a significant damage of 2nm SFT by an edge dislocation was reported in [8] and a complete absorption of overlapping non-perfect SFTs, formed in high-energy displacement cascade modeled in Cu, was observed in [13]. At least two other features of SFT-dislocation interaction 1) TEM contrast of the SFT changes when dislocation approaches and it is restored when dislocation passes through and 2) when the lower (relatively to the slip plane in Fig. 1) part of an SFT disappears due to interaction whereas the upper one remains undamaged, were experimentally observed in gold [5] and are consistent with MD studies reported here.

We admit that the SFTs studied here are more related to irradiation conditions, when the maximum of size distribution function is related to about 2.5nm, than to in-situ experiments, when the size of observed SFTs is of the order 25-50nm. Such a considerable difference in size can lead to a difference in the mechanism of dislocation-DFT interaction. Nevertheless, we conclude that some mechanisms described here are consistent with the available in-situ observations. More atomic-scale studies are necessary to clarify effects involved in plastic instability and creation of cleared channels in irradiation and non-irradiation conditions. Particularly, those for a) screw dislocations, b) SFTs of larger size, when dislocation-SFT reaction may become closer to a dislocation-(stair rod) dislocation reaction, c) lower strain rates, when the time of the interaction became long enough to involve diffusion mechanisms and d) thin film conditions (as in in-situ TEM experiments where the specimen thickness is about 100nm), when the slow moving dislocation may serve as a channel for defect (vacancy) transport to close strong sinks, e.g., surface.

References

- [1] B. N. Singh and S. J. Zinkle, *J. Nucl. Mater.* 206 (1993) 287.
- [2] J. Silcox and P. B. Hirsch, *Philos. Mag.* 4 (1959) 72.
- [3] M. Kiritani, *Mat. Sci. Eng. A* 350 (2003) 1.
- [4] J. S. Robach, I. M. Robertson, B. D. Wirth, and A. Arsenlis, *Philos. Mag.* 83 (2003) 955.
- [5] Y. Matsukawa and S. J. Zinkle, these proceedings.
- [6] M. Hiratani, H. M. Zbib, and B. D. Wirth, *Philos. Mag.* A82 (2002) 2709.
- [7] B. D. Wirth, V. V. Bulatov, and T. Diaz de la Rubia, *J. Eng. Mater. Tech.* 124 (2002) 329.
- [8] Yu. N. Osetsky, D. J. Bacon, B. N. Singh, and B. Wirth, *J. Nucl. Mater.* 307-311 (2002) 852.
- [9] Yu. N. Osetsky and D. J. Bacon, In: *Mesosopic Dynamics in Fracture Process and Strength of Materials*, IUTAM Symposium Proceedings, July 2003, Osaka, Kluwer Academic (2003) in press.
- [10] Yu. N. Osetsky and D. J. Bacon, *Modelling Simul. Mat. Sci. Eng.* 11 (2002) 427.
- [11] G. J. Ackland, G. Tichy, V. Vitek, and M. W. Finnis, *Philos. Mag. A* 56 (1987) 735.
- [12] M. Victoria, N. Baluc, C. Bailat, Y. Dai, M. I. Luppo, R. Schaublin, and B. N. Singh, *J. Nucl. Mater.* 276 (2000) 114.
- [13] B. D. Wirth, V. V. Bulatov, and T. Diaz de la Rubia, *J. Eng. Mater. Tech.* 124 (2002) 329.